

Gel-Like Lyomesophases Formed in Organic Solvents by Self-Assembled Guanine Ribbons

Tatiana Giorgi,^[a] Fabrizia Grepioni,^[c] Ilse Manet,^[a] Paolo Mariani,^{*,[b]} Stefano Masiero,^[a] Elisabetta Mezzina,^[a] Silvia Pieraccini,^[a] Letizia Saturni,^[b] Gian Piero Spada,^[a] and Giovanni Gottarelli^{*,[a]}

In memory of Jean Jacques, an excellent chemist and an extraordinary person

Abstract: Lipophilic guanosine derivatives are self-assembled into ribbonlike aggregates, both in the crystal state and in solution. The structure of the ribbons has been characterised by single-crystal X-ray diffraction and, in solution, by NMR spectroscopy and ESI-MS. Two different ribbons with different patterns of hydrogen bonds are present in the solid state and in chloroform solutions. The gel-like phases obtained in hexadecane, toluene and chloroform have been investigated by optical microscopy and small-angle X-ray diffraction: the type of phase observed is related to the molecular structure of the compounds and depends dramatically on the solvent. The structures of the phases are discussed, with the presence of the two different ribbons being taken into account.

Keywords: guanosine derivatives • liquid crystals • nucleosides • self-assembly • supramolecular chemistry

Introduction

Low molecular mass gelators of organic liquids are subjects of constant interest.^[1, 2] In contrast with their macromolecular counterparts in which covalent bonds are involved, the supramolecular organisation of these molecules, which is responsible for the gelling properties, is due to weak molecular forces including hydrogen-bonding, π -stacking and solvophobic effects. As a consequence, the process is reversible and several new applications are possible: for

example, the preparation of microcellular organic materials,^[3] porous membranes^[4, 5] and photoresponsive gels.^[6]

Owing to the difficulty in understanding the self-assembly process, and because of the variety of the structures of gelling agents, which were found almost exclusively by serendipity, often the gelling process is not completely clear;^[1] however, once a type of gelator is discovered and the polymerisation process understood, it is possible to design variations of the structure leading to interesting new properties, as for example, in urea derivatives.^[7, 8]

As gels are “easier to recognise than to define”,^[1] there are several cases in which the terms *gel* and *lyotropic liquid crystal* seem to overlap,^[1, 8–10] the only clear distinction being in the membrane field. Therefore we shall not try to find an unambiguous definition of the two states, preferring the liquid crystal name in the case of birefringent ordered structures.

In preceding work, we have described the self-assembly of lipophilic guanosine derivatives with or without added ions.^[11, 12] In the presence of ions the assembled species are columns composed of classic G-quartets,^[13] which also characterise aqueous gel structures,^[14] but when no ions are present, deoxyguanosines **1** and **2** form ribbonlike nanostructures in solution and at the solid–liquid interface. In particular, NMR work in CDCl₃ has shown the presence of two different ribbons (Figure 1): the first (ribbon I), which we hypothesised would exist in the solid state, has a definite

[a] Prof. G. Gottarelli, T. Giorgi, Dr. I. Manet, Dr. S. Masiero, Dr. E. Mezzina, Dr. S. Pieraccini, Prof. G. P. Spada
Alma Mater Studiorum—Università di Bologna
Dipartimento di Chimica Organica “A. Mangini”
Via S. Donato 15, 40127 Bologna (Italy)
Fax: (+39) 051244064
E-mail: gottarel@alma.unibo.it

[b] Prof. P. Mariani, Dr. L. Saturni
Università di Ancona, Istituto di Scienze Fisiche e INFM Istituto Nazionale per la Fisica della Materia
Via Ranieri 65, 60131 Ancona (Italy)

[c] Prof. F. Grepioni
Università di Sassari, Dipartimento di Chimica
Via Vienna 2, 07100 Sassari (Italy)

Supporting information for this article is available on the WWW under <http://www.wiley-vch.de/home/chemistry/> or from the author: ESI-MS spectra of derivative **4** and **5**; small-angle diffraction data of **1** in toluene and of **2** in chloroform and hexadecane; molecular parameters of the ribbons and structural parameters of the gel-like phases of **1**, **2**, **4** and **5**.

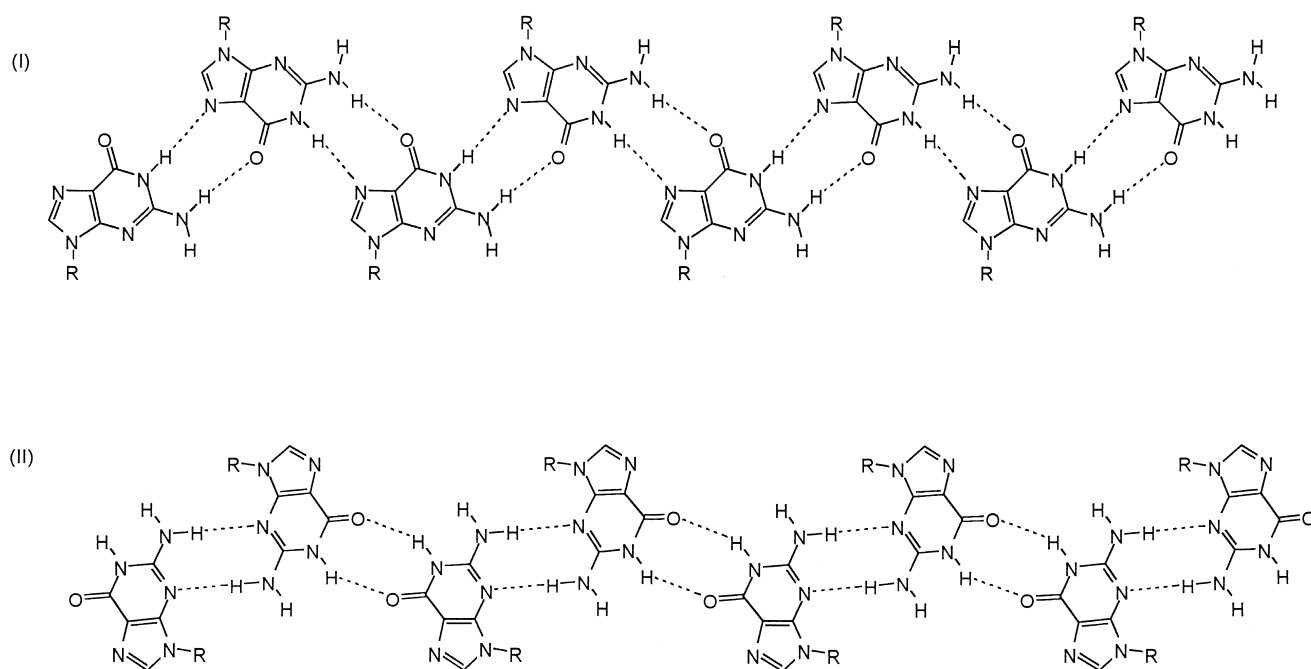
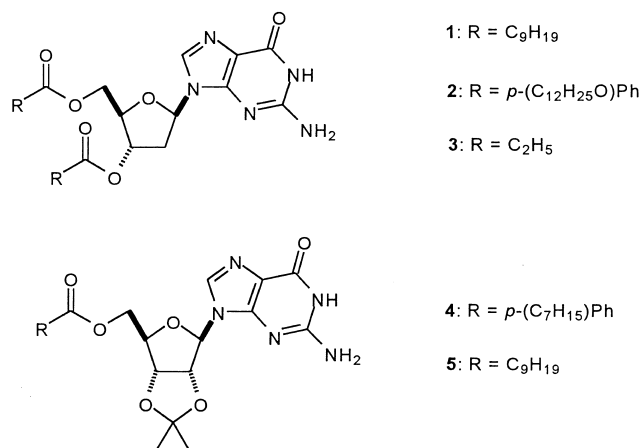


Figure 1. Hydrogen-bond pattern of the two ribbonlike assemblies of guanosine derivatives.



NMR spectrum that slowly transforms into a different spectrum corresponding to the ribbon stable in CHCl_3 solution (ribbon II); the transition from ribbon I to ribbon II is faster in the presence of moisture in the solvent.^[12] These

ribbons seem particularly interesting as their ordered molecular layers, which are obtained on solid surfaces by evaporation of the LC phase in CHCl_3 , display rectifying^[15] and photoconductive properties.^[16]

In a preliminary communication^[17] we have described a new lyomesophase formed by derivative **1** in hexadecane; more recently, Kato and co-workers have reported thermotropic^[18] and lyotropic^[19] phases formed by folic acid derivatives due to similar hydrogen-bond patterns. In this paper, we report the structure of ribbon I, obtained from single-crystal X-ray diffraction of deoxyguanosine derivative **3**, and a study of the gel-like liquid crystals formed in different solvents by derivatives **1** and **2** and by the two other guanosines **4** and **5**, which belong to the ribo series and contain the acetonide group. We believe that the variations of the gel-like structures with the chemical constitution of the gelators and with the solvent yield a good understanding of the self-assembly process leading to the gel-like phases,^[20] and that the presence of the two different ribbons in the different lyomesophases is remarkable.

Abstract in Italian: I derivati lipofili della guanosina allo stato cristallino e in soluzione sono autoassociati in aggregati a nastro. La struttura dei nastri è stata caratterizzata mediante diffrazione dei raggi X da cristallo singolo e, in soluzione, mediante NMR e ESI-MS. Allo stato solido e in soluzione cloroformica sono presenti due diversi nastri con un diverso schema di legami a idrogeno. Le fasi di tipo gel ottenute in esadecano, toluene e cloroformio sono state studiate con la microscopia ottica e la diffrazione dei raggi X a basso angolo: il tipo di fase osservata è in relazione con la struttura molecolare dei composti e dipende fortemente dal solvente presente. Vengono discusse le strutture delle fasi tenendo in considerazione la presenza dei due diversi nastri.

Results and Discussion

X-ray single-crystal study: Compound **3** crystallises in the chiral group $P1$, with two independent molecules in the asymmetric unit. The two molecules differ in the conformation of the lateral chains attached to the guanosine skeleton, as can be seen in Figure 2.

The two types of molecules interact in the solid state by means of hydrogen bonding between the guanine residues (Figure 3). The NH group of the six-membered ring interacts exclusively with the N atom of the five-membered ring ($\text{N(H)}-\text{N}$ 2.827(2) and 2.909(2) Å). The two H atoms on the NH_2 groups interact with the oxygen atom on the six-

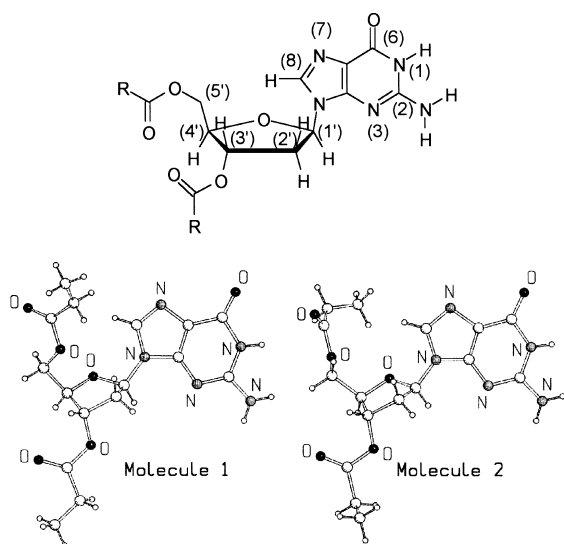


Figure 2. Ball-and-stick representation of the two independent molecules present in the asymmetric unit of crystalline **3**. Relevant bond lengths (in Å, averaged over the two molecules): N1–C2 1.357(6), N2–C2 1.339(6), C2–N3 1.334(6), N3–C4 1.359(6), C4–C5 1.379(6), C5–C6 1.422(6), N1–C6 1.411(6), C6–O6 1.211(6), C4–N9 1.365(6), C8–N9 1.363(6), C8–N7 1.310(6), C5–N7 1.410(6), N9–C1' 1.447(6), C1'–C2' 1.504(6), C2'–C3' 1.507(6), C3'–C4' 1.526(6), C4'–O4' 1.438(6), C1'–O4' 1.423(6).

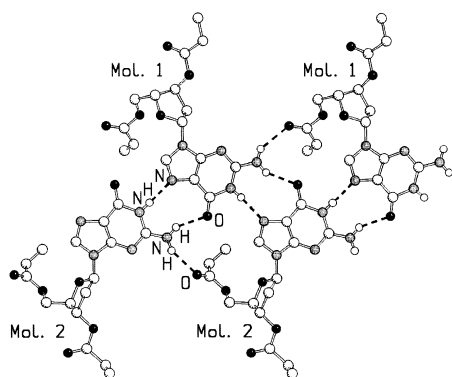


Figure 3. Ribbon formation by hydrogen-bonding interactions of the N–H...N and N–H...O type in crystalline **3**. Relevant intermolecular distances: N(H)–N 2.827(2), 2.909(2) Å; N(H)–O 2.898(2), 2.926(2), 2.984(2), 3.131(2) Å.

membered ring (N(H)–O 2.898(2) and 2.926(2) Å) and with a carbonylic oxygen belonging to the CH₂OC(O)Et lateral chains (N(H)–O 2.984(2) and 3.131(2) Å); these latter groups are flexible and can fold in order to “hook” the central part of the ribbon.

The repetition along the cell diagonal (−1 1 0) of the large tetrameric unit depicted in Figure 3 gives rise to the formation of infinite ribbons, four of which are represented in Figure 4. The guanine residues, marked in the figure by atom shading, constitute the flat central part of the ribbons, and are held together by hydrogen-bonding interactions of the N–H...N and N–H...O types shown in Figure 3. The crystal architecture results from the superimposition of the ribbons; however, the presence of the bulky lateral chains is responsible for the

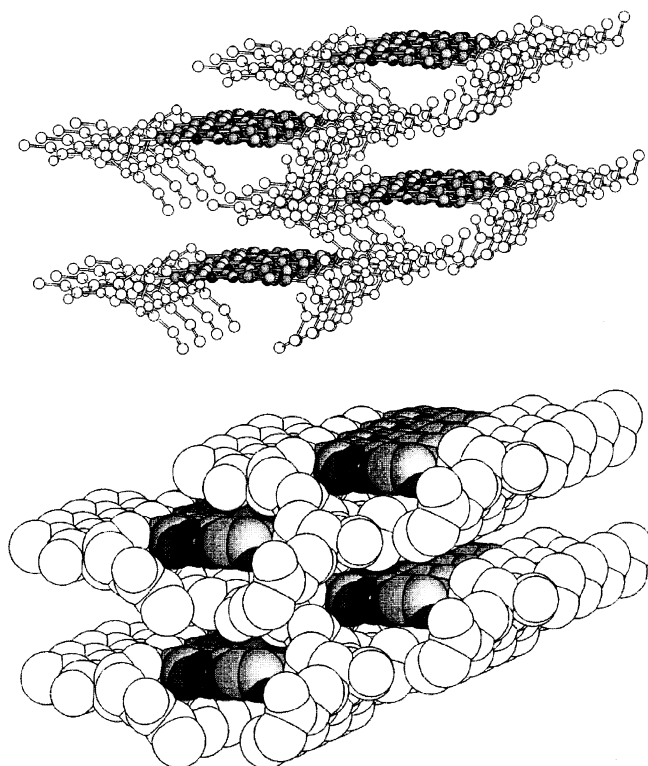


Figure 4. Shifted arrangement of the planes consisting of hydrogen-bonded guanine residues (shaded atoms) in ribbons of crystalline **3**. Top: stick-and-ball; bottom: space-filling views. For clarity H atoms are not shown.

shift observed for consecutive ribbons so that no π -stacking of the flat residues is observed (see Figure 4).

It is worth mentioning that, in the large hydrogen-bonding “rings” constituting the central part of the ribbons, the N(H)–N interactions are shorter than the N(H)–O ones within the same ring (2.827(2) versus 2.898(2), and 2.908(2) versus 2.926(2) Å). We have searched the Cambridge Crystallographic Database^[21] for neutral guanine residues forming this kind of hydrogen-bonded ring; our results are in agreement with the general observed trend.

Self-assembly in isotropic solution—spectroscopic measurements:

While for derivatives **1** and **2** the assembled structures in the solid state and in solution are completely characterised,^[12] those formed by compounds **4** and **5** require further characterisation. The ESI-MS spectra of derivatives **4** and **5** obtained from chloroform in the presence of traces of formic acid have been recorded (the most basic nitrogen which should be protonated is N(7), which is not involved in the hydrogen bonds of ribbon II, stable in chloroform). For both derivatives, assembled species up to the singly protonated heptamer can easily be detected; also signals corresponding to doubly protonated higher polymers can be seen, in the case of compound **5** up to $[5_{13}H_2]^{2+}$ (see Supporting Information).

The ¹H NMR spectrum of **5** was recorded in CDCl₃ and the signals (Table 1) were assigned by means of two-dimensional COSY and NOESY experiments. The spectrum shows a broad singlet centred at $\delta = 12.1$, corresponding to an hydrogen-bonded imino proton NH(1),^[22] which does not shift when the

Table 1. ^1H NMR data of a $2.60 \times 10^{-3} \text{ mol L}^{-1}$ solution of **5** in CDCl_3 .^[a]

	δ [ppm]	J_{HH} [Hz]
H(8)	7.59 (s)	
H(1')	5.95 (d)	1.8
H(2')	5.25 (dd)	6.3, 1.8
H(3')	4.97 (m)	
H(4')	4.42 (m)	
H(5') ^[b]	4.69 (dd)	11.2, 5.9
H(5'') ^[b]	4.12 (dd)	11.2, 6.3
N-H(1)	12.12 (brs)	
N-H(2)	6.06 (brs)	

[a] Other resonances: 2.32 (t, $J = 7.5 \text{ Hz}$, CH_2CO), 1.60 (m, 5H, acetonide CH_3 , $\text{CH}_2\text{CH}_2\text{CO}$); 1.38 (s, acetonide CH_3), 1.25 (m, 12H, CH_2); 0.86 (t, $J = 6.5 \text{ Hz}$, CH_2CH_3). [b] H(5') and H(5'') protons were not individually assigned.

solute concentration is increased. The H(8) signal is around $\delta = 7.6$ and the H(2) resonance falls from $\delta = 6.1$ to 6.3 in a concentration range of $2.6 \times 10^{-3} - 5 \times 10^{-2} \text{ mol L}^{-1}$. The sugar proton signals are well separated and appear between $\delta = 4$ and 6.^[23] The analysis of the cross-peak intensities made on the basis of a COSY experiment allows one to distinguish the single resonances of the ribose moiety. In particular, H(1')/H(2') and H(3')/H(4') are correlated by small coupling constants, while H(2') and H(3') show larger cross-peak intensities due to a larger coupling constant.

Structural information on the assembled species in solution was obtained by $^1\text{H} - ^1\text{H}$ NOESY experiments on compound **5**, and the results compared with those of a previous work on derivative **1**.^[12] For both compounds, **1** and **5**, the NH_2 signal shifts downfield when the concentration is increased, an observation that indicates progressive involvement of this group in hydrogen bonding. Ribo derivative **5** shows more extensive aggregation than **1** at room temperature in non-anhydrous CDCl_3 ; the spectra recorded at the same concentration values used for compound **1** display broader signals for all the protons (this observation agrees well with the critical concentration measured for the two families of compounds, vide infra).

NOESY data (mixing times 0.05–0.2 ms) for a 0.01 mol L^{-1} solution of **5** confirm the presence of ribbonlike self-assembled species. Ribbon II ("solution" aggregate) is prevalent in nonanhydrous CDCl_3 , and is identified by a strong intermolecular interaction between NH_2 and H(1') and a less intense cross-peak between NH_2 and H(2') protons (Figure 5). These results parallel those obtained for deoxyribo derivative **1**. Additional cross-peaks confirming the hydrogen-bonding pattern are generated by the intrinsic structure of the compound under investigation. Important intermolecular interactions between methyl protons of the acetonide ring of one molecule and the NH_2 of the one closest to it, and between the methyl protons and the H(8) of the next closest one, allow the sequential connection between three molecules and thus confirm the hydrogen-bonding framework characterising the "solution" aggregate: the former spatial interaction, $\text{CH}_3 - \text{NH}_2$, is what is expected for the relative arrangement of monomer 1 and monomer 2 in which hydrogen-bonding to N(3) is involved; the latter, $\text{CH}_3 - \text{H}(8)$, is what is expected for the relative arrangement of monomer 2 and monomer 3 in which H(1)/O(6) hydrogen-bonds are present.^[24]

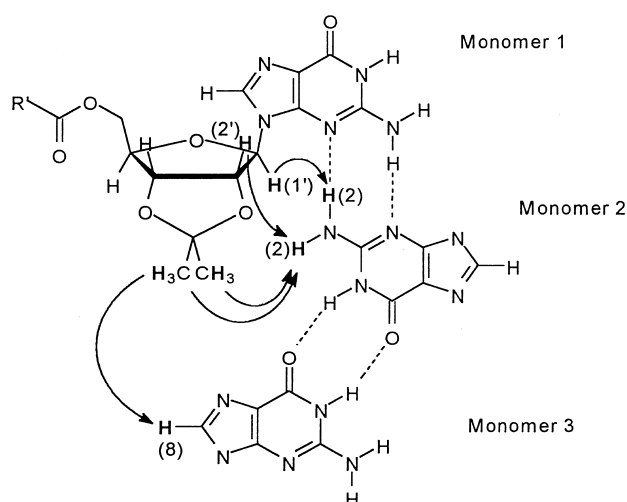


Figure 5. Important intermolecular interactions determined from NOESY experiments.

The conversion of the "crystal" aggregate (ribbon I) to the "solution" ribbon (ribbon II) in chloroform is also associated with a change in the conformation around the N(9)–C(1') glycosidic bond, as shown by NOESY experiments.^[25] It is interesting to note that in order to detect NOESY cross-peaks relating the intra- and intermolecular protons for solutions of lower concentration ($4 \times 10^{-3} \text{ mol L}^{-1}$) longer mixing times are required; this suggests the presence of shorter ribbons. The data obtained are a confirmation of the general behaviour of some lipophilic derivatives of guanosine and deoxyguanosine. These compounds self-associate, in the absence of added alkali metal ions, to give ribbonlike structures characterised by two different hydrogen-bonding networks in the solid state and in chloroform.^[26]

Circular dichroism (CD) spectra were recorded in chloroform and hexane, at different temperatures and concentrations. The spectra are, in all cases, weak and follow the shape of the absorption: no exciton patterns were detected.

Gel-like lyomesophases: The critical concentrations for the formation of the gel-like liquid-crystalline phases were determined from slowly evaporating solutions. First viscous phases were observed and then compact gel-like structures, which did not move when the test-tube was turned upside down. These phases are birefringent, indicating an ordered structure. The critical concentrations at which birefringence appears are reported in Table 2: these data are in excellent agreement with those obtained from small-angle X-ray scattering experiments. The critical values are similar for all compounds in the various solvents, with the exception of

Table 2. Critical concentration [weight %] for the formation of the gel-like phases.

Compound	CHCl_3	Toluene	Hexadecane
1	23 %	4 %	8 %
2	22 %	4 %	5 %
4	4 %	5 %	*[a]
5	4 %	5 %	*[a]

[a] * = no birefringent phases observed.

derivatives **1** and **2** in chloroform, which give the lyomesophases at much higher concentrations. The lower critical concentrations in chloroform for derivatives **4** and **5** (with respect to **1** and **2**) were expected on the basis of NMR results showing stronger aggregation for these derivatives.

IR spectra were recorded for derivative **1** as a dry film (ribbon I), and in hexadecane, toluene and chloroform (ribbon II), and the spectral region of the NH stretching has been analysed (Figure 6). The spectra for the dry film and hexadecane gel are superimposable, while in toluene the bands are slightly shifted. In chloroform the spectrum is different. These data indicate that the ribbon present in hexadecane (and possibly in toluene) must be similar to that of the solid phase and definitely different from the ribbon present in chloroform.

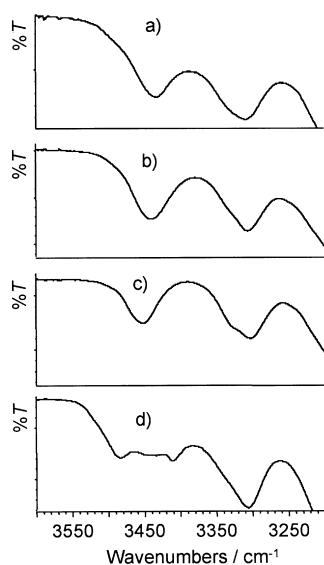


Figure 6. FT-IR spectra of **1**: a) a dry film; b) a gel-like lyomesophase in hexadecane; c) the same lyomesophase in toluene; d) an isotropic solution in chloroform.

Small-angle X-ray diffraction experiments were performed for different concentrations of the various derivatives dissolved in different solvents. Both the nature and the amount of the solvent appear to modify the scattering profile characteristics.

Gel-like phases in hydrocarbon solvents—small-angle diffraction measurements: X-ray diffraction experiments were performed in hexadecane for **2** and **1**^[17] and in toluene for **1**, **4** and **5**. In these hydrocarbon solvents, a clear dependence of the scattering profiles on the solvent concentration was detected (see Supporting Information). At concentrations lower than the critical concentration (see Table 2), the X-ray diffraction profiles show only a very broad band around $s = (5 \text{ Å})^{-1}$ ($2\theta \approx 18^\circ$), indicating the absence of order inside the sample and confirming the presence of liquid isotropic phases.

In the concentration range in which gel-like phases are observed, in the small-angle region (from which information on the long-range order can be obtained),^[27] derivatives **1** and **2** exhibit a series of narrow Bragg reflections, while a diffuse

band centred at approximately $s = (4.5 - 5 \text{ Å})^{-1}$ ($2\theta \approx 18 - 20^\circ$) is detected in the wide-angle region (which contains information on the short-range order)^[27] (Figure 7). This pattern clearly indicates that the structure combines short-range

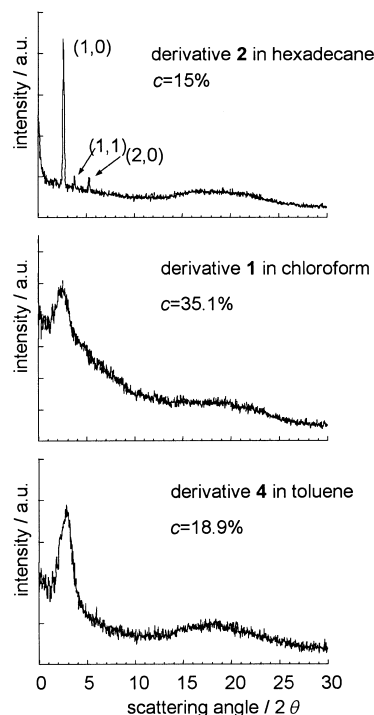


Figure 7. X-ray diffraction profiles of the gel-like phases of **2** in hexadecane, **1** in chloroform and **4** in toluene.

disorder with long-range order. However, the small-angle higher order diffractions are not easily detectable, even when very long exposure times are used. Moreover, the fading of the reflections as a function of s increases with increasing concentration. Such an effect is usually observed in lyotropic systems, as a consequence of disordering of the lattice.^[27] This indicates that the structure of this gel-like phase is intrinsically disordered, that is, it is liquid-crystalline. The analysis of the spacing ratios of the few reflections observed in the X-ray small-angle diffraction profiles gives information about the structure. The peak reciprocal spacings are in the ratio $1:\sqrt{2}:\sqrt{4}...$, indicative of a two-dimensional square packing.^[17, 27] The absence of additional small-angle peaks indicates that no correlation exists in the direction perpendicular to the two-dimensional square cell. The unit cell parameters continuously increase as a function of the solvent content, indicating a continuous swelling of the two-dimensional cell.

The investigation of the two isopropylidene derivatives **4** and **5** in toluene in the range of existence of the gel-like phases reveals the presence of a rather broad peak in the small-angle X-ray diffraction region, indicating that a certain degree of long-range order is associated with the structures occurring in these conditions (see Figure 7). For both derivatives, the peak position appears dependent on solvent concentration. The corresponding spacing moves from 60 Å to about 28 Å when the concentration increases from 5 to 20%, indicating a continuous variation of the characteristic length scale asso-

ciated with the sample structure. As for derivatives **1** and **2**, a large band is detected in the wide-angle region too, centred at about $s = (5 \text{ \AA})^{-1}$ ($2\theta \approx 18^\circ$). The absence of any other Bragg peaks indicates that the structure formed in toluene by the two derivatives in this concentration range has no crystalline long-range order. Because of the birefringence and the low degree of order, the gel-like phases observed for **4** and **5** are considered to be liquid-crystalline as well.

At higher nucleoside concentrations (ca. 20% for **2**, **4** and **5** and 10% for **1**), the gel-like structures appear to coexist with crystalline structures: the X-ray diffraction profiles are characterised by the presence of a series of intense peaks, the positions of which appear to be independent of the solvent content. A layered structure has been proposed for the dry fibre formed by derivative **1**.^[28]

Gel-like phases in chloroform—small-angle diffraction measurements: X-ray diffraction results obtained from **2**, **4** and **5** in chloroform show a different behaviour with respect to that observed in hydrocarbon solvents. Up to the critical concentrations, the X-ray beam is completely absorbed by the sample. In the concentration range in which gel-like phases are observed, the diffraction profiles are characterised by a broad peak in the small-angle region, while a diffuse band is detected in the wide-angle region, at about $s = (4.5\text{--}5 \text{ \AA})^{-1}$ ($2\theta \approx 18\text{--}20^\circ$) (see Supporting Information and Figure 7). As before, this pattern is indicative of a liquid-crystalline phase. However, in contrast with the results in hydrocarbon solvents, the position of the small-angle peak shows a rather slow dependence on the chloroform content (in the case of **2**) or does not show any dependence at all (in the case of **4** and **5**). These facts suggest that this solvent is unable to swell the structure. At high concentrations (45, 20 and 30%, for **2**, **4** and **5**, respectively), crystallisation occurs.

Structural models for the gel-like lyomesophases: The structural models for the liquid-crystalline phases observed in the different systems were analysed considering the peculiar ability of deoxyguanosines to form ribbonlike structures in the absence of ions. Accordingly, the analysis of the variation of the unit cell parameter as a function of the solvent concentration appears to be appropriate for deriving the ribbon packing model.

If we consider the presence of rod-shaped structural elements with constant cross-sectional area S packed into a two-dimensional cell, we find that the a versus c data can be fitted by different swelling models.^[27, 29, 30] Whatever the shape of the rod section, the master equation is Equation (1), in which a is the two-dimensional unit cell parameter, k is a constant, taking into account the cell symmetry (e.g., $k = \sqrt{3}/2$ for hexagonal or pseudohexagonal packing and $k = 1$ for square packing), C is the average distance between rod centres (normal to the two-dimensional cell plane), L is the average length of the rods and c_v is their volume concentration.

$$LS = Cka^2c_v \quad (1)$$

c_v can be derived from c , the weight concentration: in particular, we assume that the solvents and the different guanosine derivatives have equal specific volumes (therefore, $c = c_v$). The ratio L/C gives the fraction of solvent in the C direction. For rod-shaped elements infinite in length, L/C is one; for finite rod-shaped objects that swell isotropically (i.e. on dilution the interparticle distances increase uniformly in all three dimensions), $L/C = t/a$ (where t , which depends on the shape of the rod section and is then proportional to \sqrt{S} , is the effective radius of the rod).^[29, 30]

Equation (1) can thus be rewritten as Equation (2),^[30] in which $b = (S/k)^{1/2}$ and $\mu = -1/2$ for the $L/C = 1$ condition (infinite rods), while $b = (tS/k)^{1/3}$ and $\mu = -1/3$ for uniform isotropic swelling.

$$a = bc_v^\mu \quad (2)$$

Therefore, c_v exponents $-1/2$ and $-1/3$ can be considered as fingerprints of interparticle distances decreasing in a plane (two-dimensional swelling) or isotropically in the volume around the particles in all three dimensions (three-dimensional swelling), respectively; from parameter b , the rod cross-sectional area can be defined. If the length of the rod particles depends on the concentration or if the changes in the interparticle distances with concentration are not isotropic, the power law dependence of a on c_v can be even slower.^[30, 31]

Gel-like phases in hydrocarbon solvents: In the case of the gel-phase of **1** and **2** in hydrocarbon solvents (toluene and hexadecane, respectively; for **1** in hexadecane see ref. [17]), a two-dimensional square packing of the structure elements can immediately be deduced from the spacings of the small-angle reflections. The cell parameter increases with increasing solvent content, clearly indicating that the hydrocarbon solvents are able to penetrate the structure (see Supporting Information). The swelling behaviour is analysed by means of the assumption that the guanine residues cluster into regions from which the hydrocarbon chains are excluded and that the chains are completely dissolved in the solvent.^[17] In this way, once the ratio between the volume of the deoxyguanosine part (base and sugar) and the full volume of the derivatives (see Supporting Information) has been determined from molecular models, the cross-sectional area of the guanine core of the structure elements (S_{core}) can be derived directly from parameter b in Equation (2), which is obtained by the fitting procedure.

The a versus c_v data are well fitted by the two-dimensional swelling model ($\mu = -0.47 \pm 0.02$ and -0.49 ± 0.04 , $b = 11.1 \pm 0.5$ and $13.1 \pm 1.2 \text{ \AA}$, for **1** and **2**, respectively). From the fitting parameters, constant cross-sections S_{core} of about 50 and 46 \AA^2 can be derived (with $k = 1$) for **1** and **2**; this corresponds well to the guanine ribbon cross-section determined from the model ($S_{\text{core}}^* = 48 \pm 2 \text{ \AA}^2$). The swelling behaviour is consistent with the occurrence of a phase in which the structure elements, infinite in length and with their long axes parallel to each other, are packed in a two-dimensional square cell. The ribbons contain the guanine residues in the extended hydrogen-bonded configuration, while the hydrocarbon chains, together with the hydrocarbon solvent in which they

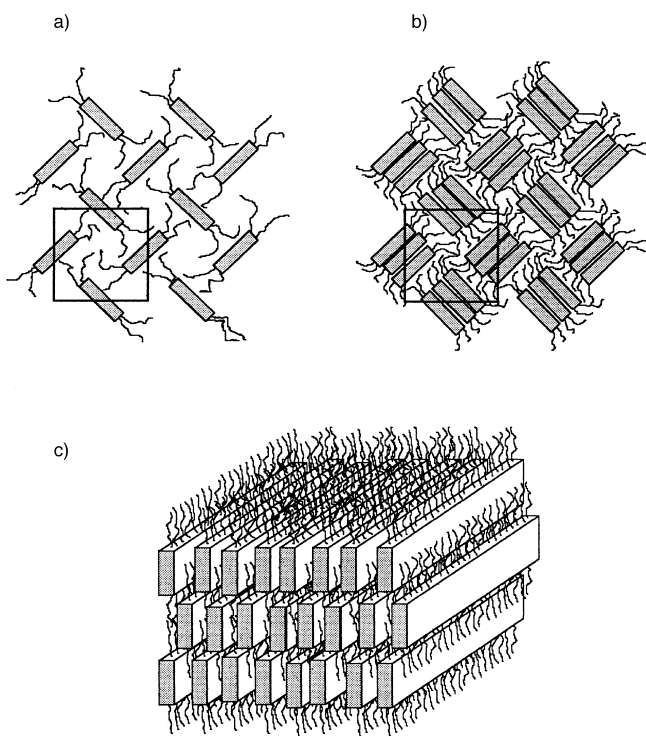


Figure 8. Models for gel-like phases in hydrocarbon solvents (a) and in chloroform (b and c).

are dissolved, fill the lateral gap between the ribbons (Figure 8a).

The diffuse band observed at $(4.5\text{--}5\text{ \AA})^{-1}$ ($2\theta \approx 18\text{--}20^\circ$) is characteristic of liquid paraffins, and indicates a disordered (liquidlike) organisation inside the hydrocarbon region. As the solvent is expected to scatter in the same region, no detailed information on the hydrocarbon conformation can be derived.

In the case of derivatives **4** and **5** in toluene, the local packing of the ribbons cannot be inferred from simple X-ray diffraction data owing to the presence of only one broad peak. However, the swelling experiments for these compounds show behaviour similar to that observed for deoxy derivatives **1** and **2**. In fact, the fit of the a versus c data to Equation (2) shows a two-dimensional swelling mode: in both cases, μ turns out to be very close to $-1/2$ ($\mu = -0.51 \pm 0.01$ and -0.53 ± 0.03 , respectively), while the cross-sectional area of the guanosine core in the ribbons (S_{core}), calculated by assuming a two-dimensional square packing of the structure elements (i.e., $k=1$) and using a value for $V_{\text{core}}/V_{\text{mol}}$ of 0.27 for **4** and of 0.30 for **5**, is 45.5 \AA^2 and 49.0 \AA^2 , respectively. The S_{core} value becomes 52.6 and 56.5 \AA^2 when a local hexagonal packing ($k=\sqrt{3}/2$) is considered. The cross-sectional area of the guanosine core of the ribbon calculated from molecular models ($S_{\text{core}}^* = 48 \pm 2\text{ \AA}^2$) is very similar to the experimentally derived values, confirming that these two derivatives, too, form ribbons in hydrocarbon solvents. The structural model for the gel-like phase in toluene is thus similar to the one proposed for derivatives **1** and **2**: the ribbons are likely to be packed in a two-dimensional cell. Together with the hydro-

carbon solvent in which they are dissolved, the hydrocarbon chains fill the lateral gap between the ribbons. As before, the broadness of the wide-angle peak indicates that the chains exhibit a liquidlike conformation.

Gel-like phases in chloroform: The structure of the gel-like phase formed in chloroform by **2** can be discussed only tentatively. In this case, only one, rather broad, Bragg peak is detected in the small-angle region. Moreover, the peak position is slowly dependent on the solvent content: the c_v exponent obtained by fitting the data with Equation (2) is $\mu = -0.11 \pm 0.01$, clearly indicating that the swelling is not isotropic.^[30] However, the L/C value calculated as a function of concentration by using Equation (1) with $S_{\text{core}}^* = 48\text{ \AA}^2$ is larger than 1. This suggests a different structure, in which the rods, packed in a two-dimensional cell (either square or hexagonal), are composed of multiple stacked ribbons: in this arrangement the solvent is not able to penetrate the ribbon regions.^[32] The chloroform thus favours self-assembly into larger fibres; however, because no evidence for phase separation has been obtained by optical microscopy observations, even after weeks, we also suggest that the individual fibres do not aggregate into specific separated domains. Assuming that the ribbons are infinitely long, the observed dimensions are compatible with a stacking of the ribbons in the range of two to four layers, depending on the concentration. Under these conditions, Equation (1) can be rewritten as $nS_{\text{core}} = Ka^2c_vV_{\text{core}}/V_{\text{mol}}$, where n is the number of stacked ribbons in the unit cell. The proposed structure is sketched in Figure 8b. Considering the observed X-ray diffraction profiles, two points should be underlined: first, the breadth of the small-angle peak implies that the structure is characterised by a low degree of long-range order; second, the absence of a Bragg peak in the wide-angle region (around the expected stacking distance of about $3.3\text{--}3.4\text{ \AA}$) is compatible with the small number of stacked layers in a fibre, but also indicates that the neighbouring stacks are arranged in a random fashion in relation to each other throughout the gel-like phase.

As for derivative **2**, the analysis of the structure of the gel-like phases formed by **4** and **5** in chloroform is only tentative. In fact, in these cases as well, the X-ray diffraction profiles are characterised by only one peak in the small-angle region, even when the profiles are obtained with extremely long exposure times; therefore, the symmetry of the phase cannot be determined. In both **4** and **5**, the peak spacing appears to be independent of solvent concentration, while the corresponding cell parameter is surprisingly small ($a = 23\text{--}24\text{ \AA}$) in comparison with that observed for **2** ($a = 35\text{--}38\text{ \AA}$). These results indicate that the packing is very tight and that chloroform is unable to penetrate the cell. In this case too, no indication of phase separation has been detected by optical microscopy observations.

Let us hypothesise that the structure is formed by guanine ribbons packed in a two-dimensional structure (square or hexagonal); the μ values obtained from fitting the a versus c data to Equation (2) are very small, that is, -0.028 and -0.023 for **4** and **5**, respectively, indicative of structure elements whose length is variable with concentration.^[30, 31] The L/C values, calculated with Equation (1) by using a

theoretical cross-sectional area of the ribbon guanosine core of 48 \AA^2 , are compatible with a model of short structure elements whose lengths change as a function of solvent content: in particular, the length of the aggregates reduces when the chloroform content increases (see also the NMR spectroscopy section).

A second structural model can be obtained by considering the formation of multiple stacked ribbons and a subsequent arrangement in a smectic fashion of separate layers containing alternately the bases and the chains (Figure 8c). In this structure, the spacing of the observed Bragg peaks corresponds to the layer repeat distance: comparison with the dimensions of molecular models indicates that complete interdigitation of the chains or a tilt of the ribbon formed by the guanine residues should occur. However, because of the absence of swelling, in this case too the length of the ribbons should be considered to be dependent on solvent concentration. This peculiar behaviour can be determined by the occurrence of large interactions between ribbons in chloroform and by the ability of this solvent to compete with hydrogen bonds. Because of the exclusion of solvent from the ribbon region, dilution will preferentially increase the end-to-end axial distance between the ribbons. At low concentration, the aggregates become very short and a very loose packing results. As expected, a phase transition to the isotropic phase occurs.

Conclusion

Lipophilic guanosine and deoxyguanosine derivatives are able to gelatinise some organic solvents, provided that a sufficiently long hydrocarbon tail is present. The process is mediated by the formation of ribbonlike assembled species, which are described both in the solid state and in solution for deoxyribo compounds **1** and **2**, while in the ribo series (compounds **4** and **5**) they are described only in solution by NMR spectroscopy and ESI-MS. The nature of the gel-like phases is strongly influenced by the structure of the solute and by the solvent.

Deoxy derivatives **1** and **2** in hydrocarbon solvents form a quite ordered lyotropic liquid-crystalline phase characterised unequivocally, from the spacing of the few small-angle diffraction peaks observed, as a two-dimensional square packing of the ribbons. Also, isopropylidene derivatives **4** and **5** in toluene form birefringent gels, which were tentatively described as likewise having a two-dimensional square disposition of the ribbons, on the basis of dilution studies and from calculation of the cross-sectional area.

In CHCl_3 the situation is rather different: the critical concentrations are drastically different for the deoxy and the ribo series; all compounds give a single small-angle diffraction peak whose position is scarcely (for derivative **2**) or not (for **4** and **5**) influenced by dilution; this is interpreted as a weakening of the hydrogen-bonded structure (detected also by NMR spectroscopy) as a result of the competitive solvent causing the breaking of the ribbons into shorter fragments. A concomitant effect could be the strong interaction of alkyl side chains of different ribbons, caused by the polar solvent; as

a consequence, new phases are observed, which are, however, different for deoxy (**1** and **2**) and ribo (**4** and **5**) derivatives.

As for the presence of ribbons I or II in the phases, ribbon II is certainly present in CHCl_3 . It is tempting, and also reasonable in the light of IR spectroscopic results, to say that ribbon I is present in hydrocarbon solvents, thus justifying on a molecular basis the claim of different phases present in these solvents. In all cases the gelling process is rather well understood and the prospective of further developments seems concrete.^[4, 6]

The liquid-crystalline phases described in this report are completely different from lyomesophases and gels formed in water^[14, 33, 34] by natural guanine nucleosides and nucleotides. The self-assembly process at the origin of the present phases does not involve alkali metal ions and leads to flat, ribbonlike structures in which the chirality of the nucleosides is not expressed at the supramolecular level.^[35, 36] CD spectra of the ribbon aggregates are very weak and almost identical to those of the monomers. The lyomesophases and gels formed in water can instead be described as stacks of G-quartets forming chiral columnar structures containing alkali metal ions. In this case there is strong chirality transfer from the monomers to the supramolecular aggregates and exciton CD are observed in the guanine absorption region.

Experimental Section

Derivatives **1**, **2** and **3** were synthesised as reported in refs. [11, 12 and 37], respectively.

2',3'-O-Isopropylidene-5'-decanoylguanosine (5): Compound **5** was prepared in 86 % yield starting from 2',3'-O-isopropylideneguanosine (Sigma) (0.77 mmol) and decanoic anhydride (1.2 equiv) according to the literature procedure.^[37] ^1H NMR (300 MHz, $[\text{D}_6]\text{DMSO}$): $\delta = 0.84$ (t, 3 H; $\text{CH}_2\text{-CH}_3$), 1.20 (m, 12 H; CH_2), 1.31 (s, 3 H; CH_3), 1.44 (m, 2 H; $-\text{CH}_2\text{-CH}_2\text{-CO}$), 1.49 (s, 3 H; CH_3), 2.26 (t, 2 H; $\text{CH}_2\text{-CO}$), 4.09–4.23 (m, 3 H; H-4', H-5', H-5''), 5.11 (dd, 1 H; H-2'), 5.25 (dd, 1 H; H-3'), 6.00 (d, 1 H; H-1'), 6.52 (brs, 2 H; NH_2), 7.84 (s, 1 H; H-8), 10.69 (brs, 1 H; NH); ES-MS: m/z (%): 478.15 (100) [$5^+ + \text{H}$].

2',3'-O-Isopropylidene-5'-(p-heptyl)benzoylguanosine (4): Adamantane-carbonyl chloride (0.55 mmol) was added to a stirred solution of Et_3N (1.84 mmol) and *p*-heptylbenzoic acid (0.61 mmol) in CH_3CN (10 mL). The resulting mixture was stirred at RT for 2 h. 2',3'-O-isopropylideneguanosine (0.46 mmol) and 4-dimethylaminopyridine (0.020 g) were then added and the resulting suspension was stirred for 72 h. Methanol (0.5 mL) was added and stirring was continued for 30 min. The suspension was filtered and the resulting solution was concentrated in vacuo. The crude reaction mixture was purified by column chromatography on silica gel (eluent: gradient $\text{CH}_2\text{Cl}_2/\text{CH}_3\text{OH}$ 97:3 \rightarrow 90:10). The product obtained was redissolved in CHCl_3 and washed several times with Millipore-grade water, affording compound **4** as a white solid in a 42 % yield. ^1H NMR (300 MHz, $[\text{D}_6]\text{DMSO}$): $\delta = 0.85$ (t, 3 H; $\text{CH}_2\text{-CH}_3$), 1.25 (m, 8 H; CH_2), 1.34 (s, 3 H; CH_3), 1.53 (s, 3 H; CH_3), 1.56 (m, 2 H; $-\text{CH}_2\text{-CH}_2\text{-Ph}$), 2.64 (t, 2 H; $\text{CH}_2\text{-Ph}$), 4.31–4.52 (m, 3 H; H-4', H-5', H-5''), 5.28 (m, 2 H; H-2' and H-3'), 6.05 (d, 1 H; H-1'), 6.56 (brs, 2 H; NH_2), 7.32 and 7.83 (m, 4 H; Ph), 7.84 (s, 1 H; H-8), 10.72 (brs, 1 H; NH); ES-MS: m/z (%): 526.31 (100) [$4^+ + \text{H}$].

Crystal structure determination: Single-crystal X-ray diffraction data for **3** were collected at room temperature on a Bruker AXS SMART diffractometer equipped with a graphite monochromator ($\text{MoK}\alpha$ radiation, $\lambda = 0.71073 \text{ \AA}$): $\text{C}_{16}\text{H}_{21}\text{N}_5\text{O}_6$, $M_r = 379.38$, triclinic, $P1$, $a = 8.903(1)$, $b = 10.327(1)$, $c = 10.796(1) \text{ \AA}$, $\alpha = 86.109(5)$, $\beta = 71.834(5)$, $\gamma = 72.496(4)^\circ$, $V = 899.1(2) \text{ \AA}^3$, $Z = 2$, $F(000) = 400$, $\mu = 0.109 \text{ mm}^{-1}$, θ range $2\text{--}34^\circ$, 13 006 reflections, 9877 independent, refinement on F^2 for 488 parameters, wR (F^2 , all reffs.) = 0.1540, R_1 [$I > 2\sigma(I)$] = 0.0540. The computer program SHELX97^[38] was used for structure solution and refinements based on F^2 .

All non-hydrogen atoms were refined anisotropically and hydrogen atoms were added in calculated positions. SCHAKAL99^[39] was used for the graphical representation of crystalline **3**. The program PLATON^[40] was used to calculate the hydrogen bonding interactions of the N–H...N and N–H...O type. CCDC-171521 contains the supplementary crystallographic data for this paper. These data can be obtained free of charge via www.ccdc.cam.ac.uk/conts/retrieving.html (or from the Cambridge Crystallographic Data Centre, 12 Union Road, Cambridge CB2 1EZ, UK; fax: (+44) 1223-336033; or deposit@ccdc.cam.ac.uk).

Spectroscopic measurements: ¹H and two-dimensional COSY spectra were measured on a Varian Gemini 300 instrument; two-dimensional NOESY experiments were carried out on a Varian Mercury 400 instrument; $\delta(\text{H})$ values quoted above are relative to the solvent peak in CDCl₃ solutions and coupling constants *J* are given in Hz. Varian Gemini 300: $\delta(\text{H})$ for 6.4×10^{-4} to $5.5 \times 10^{-2} \text{ mol L}^{-1}$ solutions; two-dimensional COSY: $4 \times 10^{-3} \text{ mol L}^{-1}$ solution. Varian Mercury 400 instrument: two-dimensional NOESY: $1 \times 10^{-2} \text{ mol L}^{-1}$ solution; the instrumental settings were: spectral width 6.0 kHz, pulse width 12.8 μs (90° flip angle), repetition time 2.5 s, complex data point in *t*₁ 1024, complex FIDs in *t*₂ 256, mixing times 0.05–0.2 s, number of transients 16.

FT-IR spectra were measured with a Nicolet Protégé 460 spectrometer.

Preparation of the phases: The liquid-crystalline phases in chloroform were obtained by slow evaporation of the solvent from isotropic solutions of the guanosine derivatives. Lyomesophases (and isotropic solutions) in hexadecane were prepared by dissolving the guanosine compound in the minimum amount of dichloromethane and adding the relevant amount of hexadecane; the chlorinated solvent was then removed under vacuum. The mesophases (and isotropic solutions) in toluene were obtained by adding the solute to the appropriate amount of solvent and heating the mixture to a clear, homogeneous solution. The critical concentrations for the formation of the gel-like phases in toluene and chloroform were determined by observation, under crossed polarisers, of the appearance of birefringence in solutions in slow evaporation. In the case of hexadecane, the critical concentrations were determined by observation of the presence or absence of birefringence in solutions of different concentration.

Small-angle X-ray diffraction measurements: Small-angle X-ray diffraction experiments were performed with a 3.5 kW Philips PW1830 X-ray generator equipped with a Guinier-type focussing camera operating in a vacuum: a bent quartz crystal monochromator was used to select the Cu_{K α} radiation ($\lambda = 1.54 \text{ \AA}$). The explored *s* range extended from 0.01 to 0.35 \AA^{-1} ($s = 2\sin\theta/\lambda$, where $2\sin\theta$ is the scattering angle). The samples were mounted in vacuum-tight cells with thin mica windows. In order to reduce the spottiness arising from possible macroscopic monodomains, the cells were continuously rotated during exposure. The sample-cell temperature was controlled to an accuracy of 0.5 °C by means of a circulating thermostat. The diffraction patterns were recorded on a stack of four Kodak DEF-392 films. In each experiment, a number of sharp or broad reflections were observed and their spacings measured following the usual procedure.^[41] In the liquid-crystalline phases, the unit cell parameter is indicated by *a*.

In some cases, the X-ray diffraction profiles were recorded after solvent loss due to partial evaporation in order to follow the general trend of the structural parameters. Therefore, in such cases, the sample concentration, which was determined by gravimetric measurements, is only indicative.

Acknowledgement

This work was supported by the University of Bologna (funds for selected topics) and MIUR (PRIN). We thank Professor T. Kato (Tokyo) for a preprint of ref. [18] and Dr. L. Brunsveld (Eindhoven) for a copy of his PhD thesis.

- [1] P. Terech, R. G. Weiss, *Chem. Rev.* **1997**, 97, 3133–3159.
- [2] J. H. van Esch, B. Feringa, *Angew. Chem.* **2000**, 112, 2351–2354; *Angew. Chem. Int. Ed.* **2000**, 39, 2263–2266.
- [3] C. Shi, Z. Huang, S. Kilic, J. Xu, R. M. Enick, E. J. Beckmann, A. J. Carr, R. E. Melendez, A. D. Hamilton, *Science* **1999**, 286, 1540–1543.

- [4] W. Gu, L. Lu, G. B. Chapman, R. G. Weiss, *Chem. Commun.* **1997**, 543–544.
- [5] R. J. Hafkamp, B. P. A. Kokke, I. M. Danke, H. P. M. Geurts, A. E. Rowan, R. J. M. Nolte, *Chem. Commun.* **1997**, 545–546; H. H. Lee, H. Lee, Y. H. Ko, Y. J. Chang, N. K. Oh, W. C. Zin, K. Kim, *Angew. Chem.* **2001**, 113, 2741–2743; *Angew. Chem. Int. Ed.* **2001**, 40, 2669–2671.
- [6] K. Murata, M. Aoki, T. Nishi, A. Ikeda, S. Shinkai, *Chem. Commun.* **1991**, 1715–1718.
- [7] J. Campbell, M. Kuzma, M. Labes, *Mol. Cryst. Liq. Cryst.* **1983**, 95, 45.
- [8] J. van Esch, F. Schoonbeek, M. de Loos, H. Kooijman, A. L. Spek, R. M. Kellogg, B. L. Feringa, *Chem. Eur. J.* **1999**, 5, 973–950.
- [9] T. Tachibana, T. Mori, K. Hori, *Nature* **1979**, 278, 578–579.
- [10] P. Terech, C. Barthet, *J. Phys. Chem.* **1988**, 92, 4269–4272.
- [11] E. Mezzina, P. Mariani, R. Itri, S. Masiero, S. Pieraccini, G. P. Spada, F. Spinozzi, J. T. Davis, G. Gottarelli, *Chem. Eur. J.* **2001**, 7, 388–395.
- [12] G. Gottarelli, S. Masiero, E. Mezzina, S. Pieraccini, J. P. Rabe, P. Samorì, G. P. Spada, *Chem. Eur. J.* **2000**, 6, 3242–3248.
- [13] These columns form cholesteric and hexagonal lyomesophases in hydrocarbon solvents: S. Pieraccini, G. Gottarelli, P. Mariani, S. Masiero, L. Saturni, G. P. Spada, *Chirality* **2001**, 13, 7–12.
- [14] J. F. Chantot, T. Haertle, W. Gushlbauer, *Biochimie* **1974**, 56, 501–507.
- [15] R. Rinaldi, E. Branca, R. Cingolani, R. De Felice, E. Molinari, S. Masiero, G. P. Spada, G. Gottarelli, A. Garbesi, *Proc. Int. Conf. Phys. Semicond.* **25th** **2001**, 279, 1615.
- [16] R. Rinaldi, E. Branca, R. Cingolani, S. Masiero, G. P. Spada, G. Gottarelli, *Appl. Phys. Lett.* **2001**, 78, 3541–3543.
- [17] G. Gottarelli, S. Masiero, E. Mezzina, S. Pieraccini, G. P. Spada, P. Mariani, *Liq. Cryst.* **1999**, 26, 965–971.
- [18] K. Kanie, T. Yasuda, S. Ujiie, T. Kato, *Chem. Commun.* **2000**, 1899–1900; K. Kanie, M. Nishii, T. Yasuda, T. Taki, S. Ujiie, T. Kato, *J. Mater. Chem.* **2001**, 2875–2886.
- [19] K. Kanie, T. Yasuda, M. Nishii, S. Ujiie, T. Kato, *Chem. Lett.* **2001**, 480–481.
- [20] For a recent determination of a gel microstructure see: B. A. Simmons, C. A. Taylor, F. A. Landis, V. T. John, G. L. McPherson, D. K. Schwartz, R. Moore, *J. Am. Chem. Soc.* **2001**, 123, 2414–2421.
- [21] F. H. Allen, O. Kennard, *Chem. Des. Autom. News* **1993**, 8, 31.
- [22] In [D₆]DMSO, where solute–solute hydrogen-bonds are weakened by competition with the solvent, the same signal falls at lower frequencies ($\delta = 10.7$).
- [23] Compound **5** tends to give an octamer composed of two G-quartets more easily than compound **1**. This aggregate is formed when the solvent used for NMR measurements (CDCl₃) contains even small amounts of sodium cation and is detected by the presence of resonances different from those of the ribbons.^[37] Octamers generated by sodium instead of potassium cations are sensitive to temperature; spectra recorded at 50 °C do not show signals relative to this species.
- [24] NOESY spectra of freshly prepared solutions also show small amounts of the hydrogen-bonded “crystal” structure I, which is characterised by cross-peaks connecting H(8) with H(1) and H(8) with H(2) intermolecularly.
- [25] The crystal structure of **3** displays a hydrogen-bond linking the 5'-carbonyl oxygen with the nonbonded H(2) proton. This arrangement forces the molecule to assume *anti* conformations around the N(9)–C(1') bond, whose dihedral angles χ (O(4')–C(1')–N(9)–C(4)) are -157.6° and -136.5° . These rotamers show intramolecular distances closer for protons H(8)/H(2') than for H(8)/H(1'). NOESY spectral data show that on passing from the “crystal” to the “solution” aggregate,^[12] the conformation changes, assuming a new *anti* arrangement in which the dihedral angle χ shifts to approximately -175° . The “solution” conformation has shorter distances for H(8)/H(1') than for H(8)/H(2') protons and this fact is well documented by the presence of NOESY cross-peaks relative to protons H(8)/H(1') of larger intensity than those relative to protons H(8)/H(2') confirms the existence of the “solution” conformation. The passage from the “crystal” to the “solution” conformation is probably connected to the breaking of the weakest C=O...H(2) hydrogen-bond caused by competition with the polar CHCl₃ solvent.
- [26] Recently, Sessler et al. have reported the formation of a G-quartet without the addition of ions for a guanosine with a bulky substituent in the 8-position. This unusual behaviour was attributed to a conforma-

- tional effect imposed by the substituent. In the present case, all the data exclude the formation of similar quartets (J. L. Sessler, M. Sathiosatham, K. Doerr, V. Lynch, K. A. Abboud, *Angew. Chem.* **2000**, *112*, 1356–1359; *Angew. Chem. Int. Ed.* **2000**, *39*, 1300–1303).
- [27] V. Luzzati, in *Biological Membranes* (Ed.: D. Chapman), Academic Press, London, **1968**, pp. 71–123.
- [28] G. Gottarelli, S. Masiero, E. Mezzina, G. P. Spada, P. Mariani, M. Recanatini, *Helv. Chim. Acta* **1998**, *81*, 2078–2092.
- [29] L. Amaral, A. Gulik, R. Itri, P. Mariani, *Phys. Rev. A* **1992**, *46*, 3548–3550.
- [30] P. Mariani, L. Q. Amaral, *Phys. Rev. E* **1994**, *50*, 1678–1681.
- [31] R. Hentschke, M. P. Taylor, J. Herzfeld, *Phys. Rev. A* **1989**, *40*, 1678; R. Hentschke, M. P. Taylor, J. Herzfeld, *Phys. Rev. Lett.* **1989**, *62*, 800.
- [32] A similar structure has been suggested for rod–coil molecules: M. Lee, B.-K. Cho, H. Kim, J.-Y. Yoon, W.-C. Zin, *J. Am. Chem. Soc.* **1998**, *120*, 9168–9179.
- [33] G. Gottarelli, G. Proni, G. P. Spada, *Liq. Cryst.* **1997**, *22*, 563–566.
- [34] G. Gottarelli, G. P. Spada, A. Garbesi, in *Comprehensive Supramolecular Chemistry*, Vol. 9—Templating, Self-Assembly and Self-Organization (Eds.: J.-P. Sauvage, M. W. Hosseini), Pergamon, Oxford (UK), **1996**, pp. 483–506.
- [35] R. J. H. Hafkamp, M. C. Feiters, R. J. M. Nolte, *J. Org. Chem.* **1999**, *64*, 412–426.
- [36] For an exhaustive review on the chirality transfer in self-assembly processes see: M. C. Feiters, R. J. M. Nolte, in *Advances in Supramolecular Chemistry*, Vol. 6 (Ed.: G. W. Gokel), JAI, Stamford, **2000**, p. 41; L. Brunsveld, Ph.D. Thesis, University of Eindhoven, **2001**.
- [37] I. Manet, L. Francini, S. Masiero, S. Pieraccini, G. P. Spada, G. Gottarelli, *Helv. Chim. Acta* **2001**, *84*, 2096–2107.
- [38] G. M. Sheldrick, SHELXL97, Program for Crystal Structure Determination, University of Göttingen, **1997**.
- [39] E. Keller, SCHAKAL99, Graphical Representation of Molecular Models, University of Freiburg, **1999**.
- [40] A. L. Spek, *Acta Crystallogr. Sect. A* **1990**, *46*, C34.
- [41] G. Gottarelli, G. P. Spada, P. Mariani, in *Crystallography of Supramolecular Compounds* (Eds.: G. Tsoucaris, J. L. Atwood, J. Lipkowski), Kluwer Academic, Dordrecht, **1996**, pp. 307–330.

Received: October 10, 2001 [F3604]